Modal-Based Anisotropy Early Warning in Wind Turbine Rotor

Ambroise Cadoret, Enora Denimal, Jean-Marc Leroy, Jean-Lou Pfister, Laurent Mevel

Available online at www.sciencedirect.com

ScienceDirect

IFAC Papers Online CONFERENCE PAPER ARCHIVE

IFAC PapersOnLine 56-2 (2023) 11699–11704

Modal-Based Anisotropy Early Warning in Wind Turbine Rotor

Ambroise Cadoret [*,**] **Enora Denimal** [**] **Jean-Marc Leroy** [*] **Jean-Lou Pfister** [*] **Laurent Mevel** [**]

[*] *IFP Energies nouvelles, 92852 Rueil-Malmaison, France (e-mails: {ambroise.cadoret,jean-marc.leroy,jean-lou.pfister}.@ifpen.fr)*

[**] *Univ. Gustave Eiffel, Inria, COSYS-SII, I4S, 35042 Rennes, France (e-mails: {enora.denimal,laurent.mevel}@inria.fr)*

Abstract: Subspace-based fault detection methods are widely used for linear time-invariant systems. For linear time-periodic systems, those methods cannot be theoretically used, due to the intrinsic assumptions associated with those methods in the context of linear time-invariant models. Based on the approximation of time-periodic systems as time-invariant ones, those methods can still be applied and adapted to perform change detection for time-periodic systems, through a Gaussian residual built upon the identified modal parameters and their estimated variances. The proposed method is tested and validated on a small numerical model of a rotating wind turbine, with detection and isolation of a blade stiffness reduction leading to rotor anisotropy.

Keywords: parameter estimation based methods for FDI, statistical methods/signal analysis for FDI, signal and identification-based methods, wind turbines, uncertainty

1. INTRODUCTION

Considering the forecasted increase in the number of wind farms in the coming years, it is important to implement reliable fault detection methods based on data collected during operation for efficient maintenance. The methods based on subspace identification for Linear Time-Invariant (LTI) - modelled structures are part of the solution. And, those methods must be extended to the in-operation rotating wind turbine rotors, modelled as Linear Time Periodic (LTP) systems.

Nowadays, it exists some fault detection methods designed for wind turbines. The first methods are focused on detecting aerodynamic or mass imbalance of the rotor through tower sensors (Kusnick et al., 2015; Cacciola et al., 2016). In these methods, the effects of the damage are sought through the change in the environmental effects on the structure. Precisely, the consequence of an imbalanced rotor is the apparition of harmonics of the rotation in the time series, due to the gravity or wind loads. The main concern with these methods is that no structural faults of the rotor can be detected. In the literature, some methods defined for the detection of structural rotor faults can be found for example in Tcherniak and Mølgaard (2017). In this method, the cross-covariance of rotor sensors is used as a damage feature through a Mahalanobis distance. The issue with this method is its sensitivity to the operational conditions that must be mitigated, as in García Cava et al. (2022). Also, this approach does not provide localization information.

For LTI systems, a fault detection method based on a local approach for change detection can be used as in Döhler et al. (2016), and its extension to deal with real-world structures has been demonstrated in Döhler et al. (2014). With this method, based on a model parametrization, it is possible to perform change isolation, corresponding to damage localization in the applicative context (Basseville et al., 2004). Moreover, the possibility to isolate any change in the parameterization can be assessed (Mendler et al., 2020). For detection and localization, the approach performs a statistical test on a data-driven residual. To be robust to environmental conditions and take advantage of the identification of an identified estimate of the modes, some recent residual was directly designed in Mendler et al. (2023), using the mode shapes identified with a subspace identification. Also, the definition of the residual has been extended with a residual function of an estimated reference (Viefhues et al., 2022). In the current paper, the proposed residual should be designed with those two considerations in mind.

The previously proposed damage detection and localization approaches cannot be used for LTP systems, as the subspace identification methods are not defined for those systems. In Cadoret et al. (2022a), it has been proven that LTP systems can be approximated as LTI systems under non-stationary inputs. Consequently, those systems can be identified with the classical identification methods, and the damage detection and localization method designed for LTI systems can be performed thanks to this model approximation.

The main contribution of this paper is the extension of the existing damage detection and localization method to LTP systems, with a residual designed with the damage-sensitive feature of the studied structure, namely a wind turbine rotor. For this purpose, the paper is organized as follows, Section 2 introduces the dynamical modeling

10.1016/j.ifacol.2023.10.529

of the LTP systems, and defines the approximation of such systems as an LTI system under non-stationary inputs. Also, it defines an associated identification method, which is needed to construct the residual used in damage detection. Then, Section 3 recalls the principle of the standard subspace damage detection and localization, and defines a new residual designed for the study of wind turbine rotors. Finally, Section 4 applies damage detection to data from a small numerical model of a wind turbine.

2. IDENTIFICATION OF A LINEAR TIME PERIODIC (LTP) SYSTEM

2.1 Dynamic model

The motion of a constant rotating wind turbine can be expressed as a linear time periodic system,

$$\mathcal{M}(t)\ddot{\xi}(t) + \mathcal{C}(t)\dot{\xi}(t) + \mathcal{K}(t)\xi(t) = v(t), \tag{1}$$

where $\xi(t) \in \mathbb{R}^m$ are the displacements of the structure at the degrees of freedom (DOF) of the system, and $\mathcal{M}(t+T) = \mathcal{M}(t)$, $\mathcal{C}(t+T) = \mathcal{C}(t)$, $\mathcal{K}(t+T) = \mathcal{K}(t)$, respectively the mass, damping and stiffness matrices. T represents the rotational period. The unknown input $v(t)$ is assumed to be a Gaussian white noise. In the following, the mechanical system is expressed in a state space form, from the definition of the state vector $x(t) \in \mathbb{R}^n$ where $n = 2m$ and the observation $y(t) \in \mathbb{R}^r$.

$$x(t) = \begin{bmatrix} \xi(t) \\ \dot{\xi}(t \end{bmatrix} \quad \text{and} \quad y(t) = C_a\ddot{\xi}(t) + C_v\dot{\xi}(t) + C_d\xi(t), \tag{2}$$

where C_a, C_v and C_d are selection matrices. A noise $w(t)$ can be added to the observation. $w(t)$ is assumed to be a Gaussian white noise. This leads to the following state space expression:

$$\begin{cases} \dot{x}(t) = A_c(t)x(t) + B_c(t)v(t) \\ y(t) = C(t)x(t) + D(t)v(t) + w(t) \end{cases}, \tag{3}$$

with

$$A_c(t) = \begin{bmatrix} 0 & I \\ -\mathcal{M}(t)^{-1}\mathcal{K}(t) & -\mathcal{M}(t)^{-1}\mathcal{C}(t) \end{bmatrix},$$
$$C(t) = \begin{bmatrix} C_d - C_a\mathcal{M}(t)^{-1}\mathcal{K}(t) & C_v - C_a\mathcal{M}(t)^{-1}\mathcal{C}(t) \end{bmatrix},$$
$$B_c(t) = \begin{bmatrix} 0 \\ -\mathcal{M}(t)^{-1} \end{bmatrix} \quad \text{and} \quad D(t) = C_a\mathcal{M}^{-1}(t).$$

All matrices are periodic with period T, with $A_c(t) \in \mathbb{R}^{n\times n}$, $C(t) \in \mathbb{R}^{r\times n}$, $B_c(t) \in \mathbb{R}^{n\times m}$ and $D(t) \in \mathbb{R}^{r\times m}$.

2.2 Modal analysis of LTP systems

The Floquet theory (Floquet, 1879) was initially intended for solving linear differential equations with periodic coefficients. From this theory, the general solution of the differential equation reads:

$$x(t) = \Phi(t, t_0)x(t_0) + \int_{t_0}^{t} \Phi(t, \tau)B_c(\tau)v(\tau)d\tau, \tag{4}$$

with $\Phi(t, t_0)$ the fundamental matrix.

From the fundamental matrix and with some mathematical operations detailed in Skjoldan and Hansen (2009), it is possible to express the homogeneous part of the observation vector $(y_h(t))$ as a finite sum of eigenmodes to obtain the description of a time-invariant system. Leading to the following Floquet mode decomposition of the observation:

$$y_h(t) = \sum_{j=1}^{n} Y_j(t) \exp(\mu_j t)\, q_j(t_0), \tag{5}$$

where $q_j(t_0)$ depends on the initial conditions, μ_j is called the characteristic exponent and $Y_j(t)$ is the amplitude of the Floquet modes of the observation and a periodic vector of period $T = \frac{2\pi}{\Omega}$, which can then be expanded into a Fourier series:

$$Y_j(t) = \sum_{l=-\infty}^{\infty} Y_{j,l} \exp(il\Omega t) \tag{6}$$

By combining Equations (5) and (6), the observation vector can be expressed as an infinite sum of terms:

$$y_h(t) = \sum_{j=1}^{n}\sum_{l=-\infty}^{\infty} Y_{j,l} \exp((\mu_j + il\Omega)\, t)\, q_j(t_0) \tag{7}$$

Significant non-zero components of the expansion of $y_h(t)$ are determined by the participation factor (Bottasso and Cacciola, 2015):

$$\phi^y_{j,l} = \frac{\|Y_{j,l}\|}{\sum_{l=-\infty}^{\infty} \|Y_{j,l}\|}. \tag{8}$$

By defining a minimal participation factor (ϕ^y_{min}) an approximation of the observation $(\hat{y}(t))$ is constructed as a finite sum of eigenmodes,

$$\hat{y}_h(t) = \sum_{(j,l),\phi^y_{j,l}\geq\phi^y_{min}} Y_{j,l} \exp((\mu_j + il\Omega)\, t)\, q_j(t_0), \tag{9}$$

then, $\hat{y}_h(t)$ can then be expressed as a sum of $\tilde{n}$ eigenmodes

$$\hat{y}_h(t) = \sum_{p=1}^{\tilde{n}} Y_p \exp(\mu_p t)\, q_p(t_0), \tag{10}$$

where each index p corresponds to a pair (j, l) and $\mu_p = \mu_j + il\Omega$. From the approximation of the observation vector, the state space expression, and the associated matrices are defined in Cadoret et al. (2022a), leading to

$$\begin{cases} z_{k+1} = \tilde{\mathbf{A}}z_k + \mathbf{B}_k v_k \\ y_k = \tilde{\mathbf{C}}z_k + \mathbf{D}_k v_k + \tilde{w}_k \end{cases}, \tag{11}$$

with z_k the state vector associated with the approximation. This system represents a linear system with constant system matrices under a non-stationary input forcing, precisely the statistical moments of the input are periodic. In Cadoret et al. (2022a) it has been proven that the homogeneous part of this kind of state space ($\tilde{\mathbf{A}}$ and $\tilde{\mathbf{C}}$ in Equation (11)) can be identified with a classical output only subspace identification method.

The Stochastic Subspace Identification (SSI) (van Overschee and de Moor, 1993) aims to identify the eigenmodes of the system through the sample correlations. Here the SSI covariance-driven is presented. First, the Hankel matrix filled with correlations must be constructed. It can be done directly from matrices gathering the observations

$$\hat{H} = \mathcal{Y}^+ \left(\mathcal{Y}^-\right)^T \in \mathbb{R}^{(p+1)r\times qr}. \tag{12}$$

Where $\mathcal{Y}^+ \in \mathbb{R}^{(p+1)r\times N}$ and $\mathcal{Y}^- \in \mathbb{R}^{qr\times N}$ are defined in van Overschee and de Moor (1993). $\hat{H}$ can be seen as the Hankel matrix filled with the correlations $\hat{R}_i$, the estimate of the correlation $R_i = \mathbb{E}\left(y_k y^T_{k-i}\right) = \tilde{\mathbf{C}}\tilde{\mathbf{A}}^{i-1}G$, where

$G = \mathbb{E}\left(z_{k+1} y_k^T\right)$. The Hankel matrix can be factorized such that $\hat{H} = O_p C_q + \mathrm{o}(1)$, where O_p denotes the observability matrix and C_q the controllability matrix.

Then from O_p, the matrix estimates of $\tilde{\mathbf{A}}$ and $\tilde{\mathbf{C}}$ are retrieved. So, the eigenmodes can be computed with the eigenvalue decomposition of $\tilde{\mathbf{A}}$, namely $\tilde{\mathbf{A}} = \Psi\left[\mu_i\right]\Psi^{-1}$. The continuous time eigenvalues λ_i are deduced from the discrete time eigenvalues μ_i by $\lambda_i = \log(\mu_i)/\Delta t$. Finally, the mode shape matrix is found from $\Phi = \tilde{\mathbf{C}}\Psi$. Those estimates define the modal signature.

3. FAULT DETECTION METHOD

3.1 Standard subspace residual

The objective of the fault detection method is to detect a change in the system parameter, represented as the vector θ, with behavior assumed as

$$\begin{aligned} &H_0 : \theta = \theta_0 \quad \text{(reference system)},\\ &H_1 : \theta = \theta_0 + \frac{\delta}{\sqrt{N}} \quad \text{(damaged system)}, \end{aligned} \tag{13}$$

where δ is unknown but fixed and N is the length of the considered signal.

The change in the parameters will be sought through a residual $\zeta \in \mathbb{R}^l$, computed from a subspace identification. The impact of a change in the parameters on the residual can be modelled as a change in the mean of the residual (Döhler et al., 2016), such that

$$\zeta \sim \begin{cases} \mathcal{N}(0, \Sigma) : H_0 \\ \mathcal{N}(\mathcal{J}\delta, \Sigma) : H_1 \end{cases}, \tag{14}$$

where $\delta \in \mathbb{R}^h$ is related to the unknown change under H_1, $\mathcal{J} = \frac{\partial \zeta}{\partial \theta}$ the sensitivity matrix of the residual with respect to the parameters and Σ the covariance matrix of the residual under both H_0 and H_1. The main assumption is that effect of the parameter change on the residual is linear, which is a good approximation for small changes. So, the detection of important changes is outside the scope of this method.

Looking at (13) and (14) together implies that, for a given statistical change δ, the more data are used, the smaller the change in the parameters can be detected. Conversely, for a given change in the parameters $\Delta\theta$, the more data are used, the higher the absolute mean of the residual will be.

Among many possibilities of Gaussian residuals, the residual was previously defined in Basseville et al. (2000) as $\zeta = \sqrt{N}\mathrm{vec}\left(U_2^T \hat{H}\right)$, with $\hat{H}$ in Equation (12) and U_2 the left null part of $\hat{H}$.

To detect a change in the distribution of the residual, the Generalized Likelihood Ratio (GLR) is used,

$$GLR(\zeta) = -2\log\frac{\sup_{\theta\in H_0} p(\zeta|\theta_0)}{\sup_{\theta\in H_1} p(\zeta|\theta)}. \tag{15}$$

As the distribution of the residual is assumed to be a Gaussian law, the GLR is defined as (Benveniste et al., 1987)

$$GLR = t = \zeta^T\Sigma^{-1}\mathcal{J}\left(\mathcal{J}^T\Sigma^{-1}\mathcal{J}\right)^{-1}\mathcal{J}^T\Sigma^{-1}\zeta, \tag{16}$$

with $\delta^* = \left(\mathcal{J}^T\Sigma^{-1}\mathcal{J}\right)^{-1}\mathcal{J}^T\Sigma^{-1}\zeta$ the value that maximise the GLR test. From this test, the Fisher matrix can be defined

$$F = \mathcal{J}^T\Sigma^{-1}\mathcal{J}. \tag{17}$$

From this matrix, it is possible to assess the impact of a change in each parameter component on the residual. The diagonal terms give the detectability of each parameter component and the non-diagonal terms quantify the impact of one parameter component on the others and vice versa.

The test is following a χ^2 distribution such as

$$t \sim \begin{cases} \chi^2(\nu, 0) : H_0 \\ \chi^2(\nu, \lambda) : H_1 \end{cases}, \tag{18}$$

where ν is the number of degrees of freedom of the distribution equal to the dimension of the parameter space, and λ is the non-centrality parameter such that

$$\lambda = \delta^T F \delta. \tag{19}$$

Based on the properties of the χ^2 distribution, the mean of the test denoted as $\bar{t}$, will be $\bar{t} = \nu$ under H_0 and $\bar{t} = \nu + \lambda$ under H_1.

From the theoretical distribution of the test (under both H_0 and H_1), it is possible *a priori* to assess the minimal change that will be detected based on a given confidence level, 95% in this paper. Here, the method defined in (Mendler et al., 2021) is used. First, the upper bound of the interval that contains 95% of the reference test $[0, t_{crit}]$ (leading to a probability of false alarm of 5%) is computed, with

$$\int_0^{t_{crit}} f_{\chi^2}(\nu, 0)(t)dt = 0.95. \tag{20}$$

Then, the minimum non-centrality parameter (λ_{min}) is defined such that

$$\int_0^{t_{crit}} f_{\chi^2}(\nu, \lambda_{min})(t)dt = 0.05 \tag{21}$$

and estimated by minimizing the following function

$$f(\lambda) = \left| \int_0^{t_{crit}} f_{\chi^2}(\nu, \lambda)(t)dt - 0.05 \right|. \tag{22}$$

Then, from Equation (19) the associated minimum statistical change can be assessed and for one parameter component

$$\delta_{h\ min} = \sqrt{\lambda_{min}/F_{hh}}, \tag{23}$$

where F_{hh} corresponds to the contribution of the h–th parameter component in the Fisher matrix. From the minimum 95%-level detectable statistical change, the associated minimum 95%-level detectable change in the h–th parameter component is

$$\Delta\theta_{h\ min} = \frac{\delta_{h\ min}}{\sqrt{N}}. \tag{24}$$

Also, from the value t_{crit} it is possible to compute the probability of detection of a statistical change δ and the associated change $\Delta\theta$ in the physical parameter θ ($\Delta\theta = \theta - \theta_0$). From the distribution of the test and the non-centrality parameter associated with the change (Equation (19)), the probability of detection (POD) is defined by

$$\mathrm{POD}(\Delta\theta) = \int_{t_{crit}}^{\infty} f_{\chi^2}\left(\nu, N\Delta\theta^T F \Delta\theta\right)(t)dt. \tag{25}$$

3.2 New residual for wind turbine rotor

As the objective is to detect a structural change in a wind turbine rotor, some specific quantities can be chosen to define a new residual. Based on previous works (Tcherniak, 2016), the phase shift and the amplitude of the rotor bending mode shapes are one of the most sensitive indicators of changes in the rotor. Those two quantities are defined as follows

$$p_j^i = \arctan\left(\frac{\Im\left(\phi_j^i\right)}{\Re\left(\phi_j^i\right)}\right) \text{ and } a_j^i = \sqrt{\Re\left(\phi_j^i\right)^2 + \Im\left(\phi_j^i\right)^2}, \tag{26}$$

with p_j^i and a_j^i respectively the phase shift and the amplitude of the j–th DOF of the i–th mode shape (ϕ_j^i). It has to be noted that one DOF has to be chosen to define the reference. In this paper the first DOF is the chosen reference, with $p_1^i = 0$ and $a_1^i = 1$ for all the mode shapes. Let us define the vector v_i that gathers the phase shifts and the amplitudes of the i–th mode shape (defined with r outputs)

$$v_i = \left[p_2^i \; p_3^i \; \dots \; p_r^i \; a_2^i \; a_3^i \; \dots \; a_r^i\right]^T. \tag{27}$$

With this vector, it is possible to express a new residual

$$\zeta_i = \sqrt{N}\left(\hat{v}_i - v_i\right) \in \mathbb{R}^{2(r-1)}, \tag{28}$$

where $\hat{v}_i$ is an estimate of v_i using a data of length N. Then, a residual that gathers the information of n mode shapes can be defined, such that

$$\zeta = \left[\zeta_1^T \; \dots \; \zeta_n^T\right]^T = \sqrt{N}\left(\hat{V} - V\right) \in \mathbb{R}^{2n(r-1)}, \tag{29}$$

where $V = \left[v_1^T \; \dots \; v_n^T\right]^T$ is the vector regrouping the phases and amplitudes of n mode shapes.

In real operational conditions, it can be difficult to know the theoretical value of V, so an estimate ($\hat{V}^0$) of this quantity in the reference state can be used instead. In this paper, an average of (n_f) different estimates is used

$$\hat{V}^0 = \frac{1}{n_f}\sum_{j=1}^{n_f}\hat{V}^{(j)}, \tag{30}$$

where $\hat{V}^{(j)}$ is an estimate of V using the j–th data set. From this, similarly to Viefhues et al. (2022), a residual ($\tilde{\zeta}$) function of the estimated reference can be defined,

$$\tilde{\zeta} = \sqrt{N}\left(\hat{V} - \hat{V}^0\right) = \zeta - \sqrt{N}\left(\hat{V}^0 - V\right). \tag{31}$$

3.3 Residual distributions

$\hat{V}$ is an estimate of V using data of length N. Then, the distribution of the residual ζ (Equation (29)) is defined by the following distribution

$$\zeta = \sqrt{N}\left(\hat{V} - V\right) \sim \begin{cases}\mathcal{N}(0,\Sigma) : H_0\\ \mathcal{N}(\mathcal{J}\delta,\Sigma) : H_1\end{cases}, \tag{32}$$

with the assumption that the effect of the parameter change on V is linear.

Now, let us take into account the estimated reference into the distribution of the residual ($\tilde{\zeta}$ in Equation (31)). First, as $\hat{V}^{(j)}$ is computed using a data set of length N

$$\sqrt{N}\left(\hat{V}^{(j)} - V\right) \sim \mathcal{N}(0,\Sigma). \tag{33}$$

As the different estimates are computed with disjointed data, they are independent, so,

$$\sum_{j=1}^{n_f}\sqrt{N}\left(\hat{V}^{(j)} - V\right) \sim \mathcal{N}(0, n_f\Sigma). \tag{34}$$

Consequently, using Equation (30) the distribution of the estimated reference is

$$\sqrt{N}\left(\hat{V}^0 - V\right) \sim \mathcal{N}\left(0, \frac{\Sigma}{n_f}\right). \tag{35}$$

Finally, as the data used for the computation of the estimates $\hat{V}$ and $\hat{V}^0$ are different, $\hat{V}$ and $\hat{V}^0$ are independent. So, the distribution of the residual $\tilde{\zeta}$ is

$$\tilde{\zeta} \sim \begin{cases}\mathcal{N}(0,\Sigma(1+1/n_f)) : H_0\\ \mathcal{N}(\mathcal{J}\delta,\Sigma(1+1/n_f)) : H_1\end{cases}. \tag{36}$$

3.4 Damage localization by fault isolation

Once the fault detection is performed, it is possible to determine the parameter component that has changed. For such purpose, the direct localization/isolation test (Basseville et al., 2000) is evaluated, where each parameter component is individually tested for change. This test assumes that the change is restricted to one statistical change component δ_h ($\mathcal{J}\delta = \mathcal{J}_h\delta_h$), where $\mathcal{J}_h$ corresponds to sensitivity of the parameter component of index h. Leading to

$$t_h = \zeta^T\Sigma^{-1}\mathcal{J}_h\left(\mathcal{J}_h^T\Sigma^{-1}\mathcal{J}_h\right)^{-1}\mathcal{J}_h^T\Sigma^{-1}\zeta, \tag{37}$$

with the following distribution

$$t_h \sim \begin{cases}\chi^2(1,0) : H_0\\ \chi^2(1,\lambda) : H_1\end{cases}, \tag{38}$$

with the degree of freedom of the damage localization test equal to one because only one parameter (denoted by h) is tested each time. For the direct test on the other parameter components (that have not changed), their respective distribution is $t_{\bar{h}} \sim \chi^2\left(1,\bar{\lambda}\right)$ under H_1, with $\bar{\lambda}$, the non centrality parameter defined as (Döhler et al., 2016)

$$\bar{\lambda} = \delta_h^2 F_{h\bar{h}}F_{\bar{h}\bar{h}}^{-1}F_{h\bar{h}}^T, \tag{39}$$

where $F_{h\bar{h}} = \mathcal{J}_h^T\Sigma^{-1}\mathcal{J}_{\bar{h}}$ and $F_{\bar{h}\bar{h}} = \mathcal{J}_{\bar{h}}^T\Sigma^{-1}\mathcal{J}_{\bar{h}}$. It means that under H_1, when the changed parameter component is tested, the test mean (denoted as $\bar{t_h}$) will be $\bar{t_h} = 1 + \lambda$, whereas $\bar{t_h} = 1 + \bar{\lambda}$ when an unchanged parameter component is tested.

4. APPLICATION: DETECTION OF STIFFNESS LOSS

Rotor anisotropy is defined as the difference of parameters (physical properties) between the blades, leading to dependent parameters. A damage detection and localization method adapted to wind turbine rotor fault has been defined, and now it will be tested on a small wind turbine model.

In this application, a theoretical model of wind turbine defined in Skjoldan and Hansen (2009) is used (see Figure 1). The model is composed of 3 DOF of blade bending, and two DOF of nacelle bending. The matrices of the system $\mathcal{M}(t)$, $\mathcal{C}(t)$ and $\mathcal{K}(t)$ are periodic matrices of period $T =$

$\frac{2\pi}{\Omega}$, with Ω the rotational speed. The model parameters are identical to those used in Skjoldan and Hansen (2009). In this example, a detection of a stiffness loss of one blade is performed, where the monitored physical parameterization consists in the stiffness of each blade, denoted G_1, G_2, and G_3, so the number of degrees of freedom, and as such the mean of the distribution of the GLR test under H_0, is $\nu = 3$. Furthermore, the residual is built using the phase shift and the amplitude of the bending modes of the rotor, which are the most damage-sensitive mode shapes, with $v_i = \left[p_2^i \; p_3^i \; a_2^i \; a_3^i\right]^T$ (see Equation (27)).

In the wind turbine field, it is common to have fixed-length data, here 600s long data sampled at 25Hz will be used.

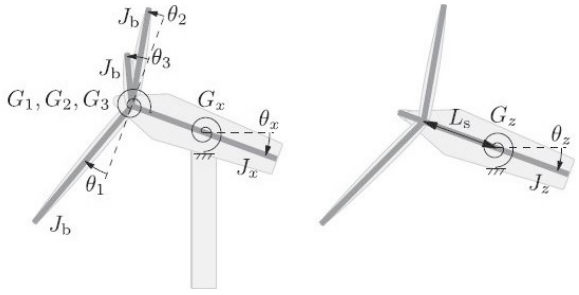

Fig. 1. Wind turbine model (Skjoldan and Hansen, 2009)

From the model matrices, the sensitivity can be computed, in this example, the first-order approximation is used. Then, the covariance matrix of the residual need to be estimated. Here the uncertainty computation method defined in Döhler and Mevel (2013) is used. Then the covariance matrices of phases and amplitudes of the mode shapes can be estimated using the method defined in Cadoret et al. (2022b). Consequently, with the sensitivity and covariance matrices, it is possible to estimate the minimum 95%-level detectable parameter change (Equation (24)) and estimate the probability of detection of specific changes (Equation (25)), as a function of the number of data sets used for the estimation of the reference (n_f in Equation (30)).

Table 1. Minimum 95%-level detectable change ($\overline{\Delta\theta}_{min}$) and probabilities of detection (POD) function of the number of data sets used for the estimation of the reference

n_f	$\overline{\Delta\theta}_{min}$	POD(1.5%)	POD(2%)	POD(2.5%)
5	1.94%	77.24%	96.12%	99.74%
10	1.86%	81.09%	97.43%	99.88%
25	1.81%	83.44%	98.08%	99.93%
50	1.79%	84.22%	98.27%	99.94%
100	1.78%	84.61%	98.37%	99.95%
200	1.78%	84.80%	98.41%	99.95%

In Table 1, the minimum 95%-level detectable parameter change and the probability of detection of different changes in the parameters are assessed. For simplicity, the relative change in one parameter component ($\overline{\Delta\theta} = \Delta\theta/\theta_0$) will be used until the end of the paper. With Table 1, it can be seen that increasing the accuracy of the reference estimate has an impact on the minimum 95%-level detectable parameter change (which is the same for all the parameter components) and on the probabilities of detection. But it can be seen that from $n_f = 25$, increasing furthermore the accuracy of the reference does not improve significantly the minimum 95%-level detectable parameter change and the POD estimations, with a maximum gain of 0.03% on $\overline{\Delta\theta}_{min}$. So for the rest of the paper, a reference estimated with $n_f = 25$ will be used. Also, the minimum identifiable parameter change and the probability of detection are coherent. As 1.5% is below $\overline{\Delta\theta}_{min}$, the probability of detection is below 95%, in contrast 2% and 2.5% are higher than $\overline{\Delta\theta}_{min}$, with an associated POD higher than 95%.

The minimum 95%-level detectable parameter change and the probability of detection have been assessed. Now, damage detection will be performed to validate the previous theoretical study. To do so, the test is performed on data corresponding to 4 states of the model, namely the reference one and three different damaged states, with a graduated stiffness reduction of G_3, precisely 1.5%, 2%, and 2.5%.

After performing the damage detection test (1000 times per damaged state), the parameter change is detected 790 times for the first damaged state, 973 times for the second, and 999 times for the third, with respective empirical POD of 79.0%, 97.3%, and 99.9%. Those results are in agreement with the theoretical POD computed *a priori* (see Table 1 at $n_f = 25$) for $\overline{\Delta G_3} = 2\%$ and 2.5%. For $\overline{\Delta G_3} = 1.5\%$, the empirical POD is lower than the theoretical one, it might be due to the value of the simulated change being lower than the 95%-level detectable parameter change. Also, with the histograms of those tests, it is possible to compare them with the theoretical distributions of the tests, see Figure 2. With this figure, it can be seen, that for each state of the structure, the histograms of the tests are matching with the theoretical distributions. Also, the mean of the tests can be studied. In Table 2, the theoretical and empirical means are compared. For the different structure states, the theoretical and empirical means are close, which confirms the theoretical statistical modeling. Consequently, from the probabilities of detection, the histograms, and the tests means, the damage detection test is assessed to perform as predicted.

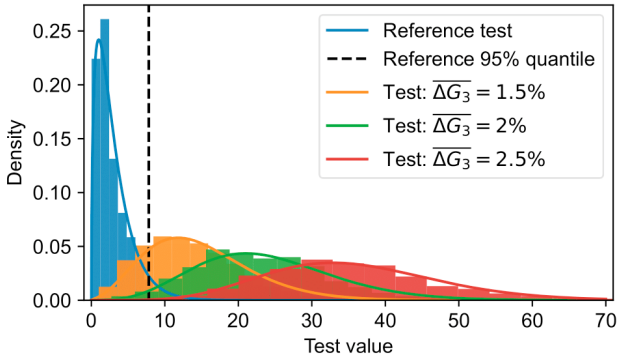

Fig. 2. Comparison of the theoretical distributions and the histograms of the damage detection tests

Table 2. Theoretical and empirical means of the damage detection tests, $\bar{t}_{th}$ and $\bar{t}_{emp}$ respectively

	Reference	$\overline{\Delta G_3} = 1.5\%$	2%	2.5%
$\bar{t}_{th}$	3	14.83	24.03	35.86
$\bar{t}_{emp}$	2.79	13.67	22.94	35.25

To finish the application, the damage localization is performed. Two cases can be studied, one with a POD lower than 95% ($\overline{\Delta G_3} = 1.5\%$) and one with a POD higher than 95% ($\overline{\Delta G_3} = 2\%$). In Table 3, the means of the localization tests corresponding to 1.5% and 2% of stiffness loss of the third blade are compared with the theoretical means. One can see that in both cases, the empirical and theoretical means are close. Consequently, it confirms that the localization test means is coherent with the theoretical distribution for all considered cases. So, the localization test is performing as it theoretically should.

Table 3. Theoretical and empirical means of the damage localization tests, $\bar{t}_{h\ th}$ and $\bar{t}_{h\ emp}$ respectively, function of the tested parameters

Simulated damage	Tested parameter	G_1	G_2	G_3
$\overline{\Delta G_3} = 1.5\%$	$\bar{t}_{h\ th}$	3.66	4.61	12.83
	$\bar{t}_{h\ emp}$	3.36	3.88	11.67
$\overline{\Delta G_3} = 2\%$	$\bar{t}_{h\ th}$	5.72	5.63	22.03
	$\bar{t}_{h\ emp}$	5.50	6.29	20.89

5. CONCLUSION

In this paper, based on the approximation of the linear time periodic system established recently and the selection of a sensitive parameterization, it has been possible to define a new residual following the guidelines of the former subspace-based damage detection methods for the rotating wind turbine rotors. Then this new residual has been extended with an expression function of an estimated reference, which makes it easier to be computed in real conditions. Finally, damage detection and localization procedures have been tested and validated, with an example on a small model of wind turbine.

REFERENCES

Basseville, M., Abdelghani, M., and Benveniste, A. (2000). Subspace-based fault detection algorithms for vibration monitoring. *Automatica*, 36(1), 101–109.

Basseville, M., Mevel, L., and Goursat, M. (2004). Statistical model-based damage detection and localization: subspace-based residuals and damage-to-noise sensitivity ratios. *Journal of sound and vibration*, 275(3-5), 769–794.

Benveniste, A., Basseville, M., and Moustakides, G. (1987). The asymptotic local approach to change detection and model validation. *IEEE Transactions on Automatic Control*, 32(7), 583–592.

Bottasso, C.L. and Cacciola, S. (2015). Model-independent periodic stability analysis of wind turbines. *Wind Energy*, 18(5), 865–887.

Cacciola, S., Agud, I.M., and Bottasso, C.L. (2016). Detection of rotor imbalance, including root cause, severity and location. In *Journal of Physics: Conference Series*, 072003. IOP Publishing.

Cadoret, A., Denimal, E., Leroy, J.M., Pfister, J.L., and Mevel, L. (2022a). Linear time invariant approximation for subspace identification of linear periodic systems applied to wind turbines. In *SAFEPROCESS 2022-11th IFAC Symposium on Fault Detection, Supervision and Safety for Technical Processes*, volume 55, 49–54. Elsevier, Pafos, Cyprus.

Cadoret, A., Denimal, E., Leroy, J.M., Pfister, J.L., and Mevel, L. (2022b). Mode shape phase change detection in wind turbine under anisotropy variation. In *ISMA 2022-International Conference on Noise and Vibration Engineering*. Leuven, Belgium.

Döhler, M., Hille, F., Mevel, L., and Rücker, W. (2014). Structural health monitoring with statistical methods during progressive damage test of s101 bridge. *Engineering Structures*, 69, 183–193.

Döhler, M. and Mevel, L. (2013). Efficient multi-order uncertainty computation for stochastic subspace identification. *Mechanical Systems and Signal Processing*, 38(2), 346–366.

Döhler, M., Mevel, L., and Zhang, Q. (2016). Fault detection, isolation and quantification from gaussian residuals with application to structural damage diagnosis. *Annual Reviews in Control*, 42, 244–256.

Floquet, G. (1879). Sur la théorie des équations différentielles linéaires. In *Annales Scientifiques de L'École Normale Supérieure*, volume 8, 3–132.

García Cava, D., Avendaño-Valencia, L.D., Movsessian, A., Roberts, C., and Tcherniak, D. (2022). On explicit and implicit procedures to mitigate environmental and operational variabilities in data-driven structural health monitoring. In *Structural Health Monitoring Based on Data Science Techniques*, 309–330. Springer.

Kusnick, J., Adams, D.E., and Griffith, D.T. (2015). Wind turbine rotor imbalance detection using nacelle and blade measurements. *Wind Energy*, 18(2), 267–276.

Mendler, A., Döhler, M., Ventura, C., and Mevel, L. (2020). Clustering of Redundant Parameters for Fault Isolation with Gaussian Residuals. In *IFAC 2020 - 21st International Federation of Automatic Control World Congress*. Berlin, Germany.

Mendler, A., Döhler, M., and Ventura, C.E. (2021). A reliability-based approach to determine the minimum detectable damage for statistical damage detection. *Mechanical Systems and Signal Processing*, 154, 107561.

Mendler, A., Greś, S., Döhler, M., and Keßler, S. (2023). On the probability of localizing damages based on mode shape changes. In *European Workshop on Structural Health Monitoring*, 233–243. Springer.

Skjoldan, P.F. and Hansen, M.H. (2009). On the similarity of the coleman and lyapunov–floquet transformations for modal analysis of bladed rotor structures. *Journal of Sound and Vibration*, 327(3), 424–439.

Tcherniak, D. (2016). Rotor anisotropy as a blade damage indicator for wind turbine structural health monitoring systems. *Mechanical Systems and Signal Processing*, 74, 183–198.

Tcherniak, D. and Mølgaard, L.L. (2017). Active vibration-based structural health monitoring system for wind turbine blade: Demonstration on an operating vestas v27 wind turbine. *Structural Health Monitoring: An International Journal*, 16(5), 536–550.

van Overschee, P. and de Moor, B. (1993). Subspace algorithms for the stochastic identification problem. *Automatica*, 29(3), 649–660.

Viefhues, E., Döhler, M., Hille, F., and Mevel, L. (2022). Statistical subspace-based damage detection with estimated reference. *Mechanical Systems and Signal Processing*, 164, 108241.